YUKONITE FROM THE GROTTA DELLA MONACA CAVE, SANT'AGATA DI ESARO, ITALY: CHARACTERIZATION AND COMPARISON WITH COTYPE MATERIAL FROM THE DAULTON MINE, YUKON, CANADA

Anna GARAVELLI, Daniela PINTO and Filippo VURRO[§]

Dipartimento Geomineralogico, Università di Bari, Via E. Orabona 4, I–70125 Bari, Italy

Marcello MELLINI and Cecilia VITI

Dipartimento di Scienze della Terra, Università di Siena, Via Laterina 8, I–53100 Siena, Italy

Tonci BALIĆ-ŽUNIĆ

Department of Geography and Geology, University of Copenhagen, Øster Volgade 10, DK-1350 Copenhagen K, Denmark

Giancarlo DELLA VENTURA

Dipartimento di Scienze Geologiche, Università di Roma Tre, Largo S. Leonardo Murialdo 1, I-00146 Rome, Italy

Abstract

We report the first Italian occurrence of yukonite, a rare hydrated arsenate of calcium and ferric iron, from Grotta della Monaca cave, S. Agata di Esaro, Cosenza, Italy. We have studied samples of cotype yukonite from the Daulton mine, Yukon, Canada, for comparison. At Grotta della Monaca, yukonite occurs in compact masses, dark reddish brown to brownish yellow in color. At the TEM scale, it consists of a chaotic assemblage of small grains (maximum dimension <20 nm) embedded in an amorphous matrix, occasionally admixed with scorodite. SAED patterns of these grains consist of weak and diffuse diffraction rings, indicating low crystallinity, and preventing any definition of symmetry or lattice parameters. Results of a combination of microanalytical, spectroscopic and thermogravimetric techniques provide chemical compositions: $Ca_{1.76}Fe^{2+}_{0.09}Fe^{3+}_{3.12}$ $[(As_{0.81}Si_{0.10}P_{0.09})O_4]_3(OH)_{3.76} \bullet 4H_2O$ for yukonite from Grotta della Monaca and $Ca_{1.76}Fe^{2+}_{0.10}Fe^{3+}_{3.56}[(As_{0.89}Si_{0.08}P_{0.03})O_4]_3(OH)_{5.16} \bullet 3H_2O$ for yukonite from the Daulton mine, close to the stoichiometry $Ca_2Fe_3(AsO_4)_3(OH)_4 \bullet 4H_2O$. The thermogravimetric data indicate a total H_2O content of ~17 wt%; FTIR data show that most of this occurs as H_2O, but some OH could be present as well. The FTIR data show, in addition, the presence of ammonium and organic matter, suggesting that poorly crystalline organic matter is trapped in the material examined. Both chemical and XRD data point to a close relation with arseniosiderite $[Ca_2Fe_3(AsO_4)_3O_2 \bullet 3H_2O]$. Both occur as oxidation products of As-bearing sulfides and seem to be composed of basically the same type of layers; arseniosiderite represents a fully crystalline substance, whereas yukonite is a semicrystalline material with a large variation in composition due to the admixture of amorphous material.

Keywords: yukonite, TEM investigation, arsenic minerals, Grotta della Monaca, southern Italy.

Sommaire

Nous décrivons ici le premier exemple connu en Italie de la yukonite, rare arsenate hydraté de calcium et de fer, provenant de la caverne Grotta della Monaca, à S. Agata di Esaro, région de Cosenza. Pour fins de comparaisons, nous avons étudié un échantillon cotype de la yukonite provenant de la mine Daulton, au Yukon, Canada. A la Grotta della Monaca, la yukonite se présente en masses compactes brun rougeâtre foncé à jaune brunâtre. A l'échelle d'observation de la microscopie électronique par transmission, la yukonite semble un amas chaotique de petits grains de dimension maximale <20 nm dans une matrice amorphe, localement avec scorodite. Les spectres de diffraction d'électrons de ces grains font preuve d'anneaux de diffraction flous et de faible intensité, indication d'une faible cristallinité, et sans potentiel pour définir la symétrie ou les paramètres réticulaires de la yukonite. Les résultats d'une combinaison de techniques microanalytiques, spectroscopiques et thermogravimétriques ont donné la composition chimique: $Ca_{1.76}Fe^{2+}_{0.09}Fe^{3+}_{3.12}$ $[(As_{0.81}Si_{0.10}P_{0.09})O_4]_3(OH)_{3.76} \bullet 4H_2O$ pour la yukonite de Grotta della Monaca, et $Ca_{1.76}Fe^{2+}_{0.10}Fe^{3+}_{3.56}[(As_{0.89}Si_{0.08}P_{0.03})O_4]_3(OH)_{5.16} \bullet 3H_2O$ pour celle de la mine Daulton. Les compositions se

[§] *E-mail address*: f.vurro@geomin.uniba.it

rapprochent de la stoechiométrie $Ca_2Fe_3(AsO_4)_3(OH)_4\cdot4H_2O$. Les données thermogravimétriques indiquent une teneur totale en H_2O d'environ ~17% (poids); les données d'absorption infrarouge (avec transformation de Fourier, FTIR) montrent que la plupart de cette quantité est vraiment H_2O, mais qu'une fraction pourrait être sous forme de OH. Les données FTIR montrent, de plus, la présence d'ammoniaque et de matière organique, ce qui fait penser que cette matière organique, à faible cristallinité, est piégée dans les matériaux examinés. Les données diffractométriques et chimiques établissent un lien étroit avec l'arséniosidérite [$Ca_2Fe_3(AsO_4)_3O_2\cdot3H_2O$]. Les deux minéraux sont produits lors de l'oxydation de sulfures arséniés, et semblent composés des mêmes types de couches. L'arséniosidérite serait une substance bien cristallisée, tandis que la yukonite serait un minéral semi-cristallin à composition variable à cause du mélange avec la matière amorphe.

(Traduit par la Rédaction)

Mots-clés: yukonite, microscopie électronique à transmission, minéraux d'arsenic mine, Grotta della Monaca, sud de l'Italie.

INTRODUCTION

Yukonite is a hydrated arsenate of calcium and iron, occurring as an alteration of As-rich minerals such as arsenopyrite (Pieczka *et al.* 1998), köttigite and parasymplesite (Dunn 1982) in Ca-rich oxidizing environments. It was originally described from Tagish Lake, Yukon, Canada (Tyrrell & Graham 1913) and later found at the Sterling Hill mine, Ogdensburg, New Jersey, U.S.A. (Dunn 1982), at Saalfeld, Thüringen, Germany (Ross & Post 1997) and in the Rędziny dolostone deposit, Sudetes, Poland (Pieczka *et al.* 1998). Recently, yukonite has been reported in mine tailings as a replacement product of arsenopyrite and scorodite (Paktunc *et al.* 2003) and from the As-rich calcareous deposits around the Nalychevskie hot springs, Kamchatka, Russia (Nishikawa *et al.* 2006).

A number of different chemical formulas have been proposed for yukonite: $Ca_6Fe_{16}(AsO_4)_{10}(OH)_{30}\cdot23H_2O$ (Jambor 1966), $Ca_2Fe_5(AsO_4)_4(OH)_7\cdot7H_2O$ (Nickel & Nichols 1991), $(Ca_{6.44}K_{0.13}Mg_{0.23})(Fe_{14.68}Al_{0.36})(AsO_4)_9O_{15.78}\cdot25.5H_2O$ (Ross & Post 1997), $Ca_7Fe_{15}(AsO_4)_9O_{16}\cdot25H_2O$ (Nickel & Nichols 2007), and $Ca_2Fe^{3+}{}_3(AsO_4)_3(OH)_4\cdot4H_2O$ (Back & Mandarino 2008). Apparently, the most recent studies converge toward the end-member formula $Ca_2Fe_3(AsO_4)_3(OH)_4\cdot4H_2O$, with up to 43% of the As possibly replaced by Si and charge-balanced by a variable OH:H_2O ratio (Nishikawa *et al.* 2006). The possible role of yukonite in stabilizing As in mine wastes, in particular from the processing of gold ores, has been considered by Paktunc *et al.* (2004).

During the characterization of the mineral assemblage occurring in the prehistorically exploited copper–iron mine at Grotta della Monaca cave, Sant'Agata di Esaro, Cosenza, Italy, a new occurrence of yukonite was discovered. The sample was investigated by a multianalytical approach, and compared with yukonite from the Daulton mine, Tagish Lake, Yukon Territory, Canada (ROM No M49312, possible type material, deposited by J.B. Tyrrell), kindly placed at our disposal by the Royal Ontario Museum of Toronto.

BACKGROUND INFORMATION

The TEM investigations performed on specimens from Nalychevskie and Venus mine, Yukon Territory, Canada, revealed that yukonite from Nalychevskie forms extremely thin (~5 nm) single plates, coexisting with amorphous material of similar composition (Nishikawa *et al.* 2006). Electron-diffraction patterns indicate that most plates have an orthorhombic symmetry, but some are hexagonal. The orthorhombic cell is C-centered with $a_{orth} = \sqrt{3}\ a_{hex} = 19.6$ Å, $b_{orth} = b_{hex}$, and corresponds to the orthohexagonal setting of the hexagonal lattice. High-resolution images of edge-on mounts indicate a periodicity normal to the plates, $d_{001} = 11.2$ Å (Nishikawa *et al.* 2006). According to these authors, yukonite from the Venus mine occurs as aggregates of irregularly bent, randomly distributed plates.

OCCURRENCE

Grotta della Monaca is a natural karst cave (~600 m a.s.l., ~300 m in length) located in the municipal district of Sant'Agata di Esaro, near Cosenza, southern Italy (Fig. 1). The cave is situated in the northern sector of the so-called Calabria–Peloritani Arc, one of the most important regions of southern Italy in terms of mineral occurrences (Bonardi *et al.* 1982). In Calabria, the formation and distribution of ore assemblages are the result of a polymetamorphic geological evolution (Lorenzoni *et al.* 1982). In particular, the Grotta della Monaca cave lies in the San Donato Unit where, according to Bonardi *et al.* (1982), an episode of mineralization connected with the Alpine cycle occurred, leading to barite, cinnabar, pyrite, galena, and chalcopyrite. These mineralized assemblages occur in the clastic sediments of the Miocene deposits also.

The most common minerals of the Grotta della Monaca cave are those typical of karstic environments. According to Dimuccio *et al.* (2005), calcite is the most common; it occurs in various forms as massive types, forming the walls of the cave. Minor amounts of other

F<small>IG</small>. 1. Location of the "Grotta della Monaca" cave, Sant'Agata di Esaro, Cosenza, Italy.

carbonates such as aragonite, dolomite, malachite and azurite have been identified in the deposit, together with yukonite, goethite, lepidocrocite, limonite, gypsum, apatite-(CaOH) and sampleite. The rare Cu-rich silicate plancheite, $Cu_8[(OH)_4Si_8O_{22}]•H_2O$, was also found in very small amounts (Dimuccio *et al.* 2005).

Owing to the abundance of metallic minerals, Grotta della Monaca cave was intensively mined beginning in the second half of the third millennium B.C. (Geniola & Vurro 2005). Visible signs of prehistoric mining activity are still evident in forms of traces of excavations along the walls of the cave and in several piles of stones. Mined materials consisted mostly of oxides and hydroxides (goethite and lepidocrocite), malachite and azurite. In addition, deposits of bat guano cover completely the floor of the inner part of the cave; they were largely used in the past as a source of agricultural fertilizer.

Yukonite, which is the object of this work, occurs as compact masses, dark reddish brown to brownish yellow, in some cases with a noticeable violet tint. Where broken, these masses show an evident conchoidal fracture, commonly lined with Ca phosphates or, subordinately, Fe oxides stained with a thin yellowish coating.

A<small>NALYTICAL</small> M<small>ETHODS</small>

The yukonite masses were crushed and separated under the stereomicroscope in order to obtain clean material for investigation. Scanning electron microscopy coupled with energy-dispersive spectroscopy (SEM–EDS) was carried out using a S360 Cambridge SEM and an Oxford–Link Ge ISIS EDS equipped with a Super Atmosphere Thin Window. Operating conditions were: 15 kV accelerating potential, 500 pA probe current, 2500 cps as average counts on the whole spectrum, count time 100 seconds. Analytical errors were 0.5% for concentrations above 15 wt%, 1% for concen-

trations of about 5 wt%, and <20% for concentrations near the detection limit. The accuracy of the analytical data was also checked using several standard minerals provided by Micro-Analysis Consultants Ltd. (U.K.).

Electron-microprobe analyses (EMPA) were made using a Cameca SX50 instrument. Operating conditions were: voltage 15 kV, beam current 15 nA; standards: $CaSiO_3$ (Ca, $K\alpha$), $BaSO_4$ (Ba, $L\alpha$), MgO (Mg, $K\alpha$), metallic arsenic (As, $L\alpha$), Fe_3O_4 (Fe, $K\alpha$), apatite (P, $K\alpha$), $CaSiO_3$ (Si, $K\alpha$), Al_2O_3 (Al, $K\alpha$).

Transmission electron microscopy (TEM) was performed with a JEOL 2010 microscope, working at 200 kV and equipped with an Oxford ISIS energy-dispersive X-ray spectrometer (EDS). Samples were finely crushed, dispersed in acetone and deposited on Cu mesh grids, previously covered by a carbon film. The grids were then covered by a further carbon film.

Thermogravimetry was performed for all the specimens with a Netzsch thermal apparatus (working conditions: sample weight 2 g, heating rate 10°/min, temperature range 20–1000°C).

Micro-FTIR spectra (Fourier transform infrared spectroscopy) were obtained on randomly oriented fragments ~30 μm thick. The spectra were collected, with a nominal resolution of 4 cm^{-1}, in transmission mode with a Nicolet Magna 760 spectrometer, equipped with a NicPlan FTIR microscope, using a KBr beamsplitter, and a nitrogen-cooled MCT-A detector. The beam diameter was 100 μm, and 128 scans were averaged for both background and sample. The spectra in digital form are available from the Depository of Unpublished Data on the MAC website [document Yukonite CM47_39].

X-ray powder-diffraction (XRD) patterns were collected using a Huber–Guinier diffractometer operated with Cu$K\alpha_1$ radiation. Background removal, smoothing and determination of diffraction maxima were performed using the program E<small>VA</small> (product of Bruker–AXS).

A chemical characterization of the surface was performed by means of X-ray photoelectron spectroscopy (XPS) using a Thermo VG Theta Probe spectrometer equipped with a micro-spot monochromatized Al$K\alpha$ source (spot size 400 µm) and a channel-plate detector. Data analysis and curve-fit procedures were carried out using the Thermo Avantage software (version 3.28).

RESULTS

Optical and SEM microscopy

Under the stereomicroscope, the Grotta della Monaca yukonite is translucent and reddish, with a resinous luster. Intense cracking and fracturing generated irregular surfaces. Cracks were evident also in back-scattered electron images, which showed polygonal-like fractures, possibly indicative of dehydration (Fig. 2a). A low-magnification, back-scattered electron image of yukonite from Grotta della Monaca is given in Figure 2b. It clearly indicates that yukonite fragments have a granular texture and show a close association of bright and dark grains.

According to the results of SEM–EDS and EMPA analyses (Table 1), this finding could be ascribed to the wide variation in compositions of the samples and, in particular, to differences in H_2O content.

TEM observations

The Grotta della Monaca yukonite mostly consists of a chaotic assemblage of small grains, less than 20 nm in diameter and with SAED (selected-area electron diffraction) patterns consisting of weak and diffuse diffraction rings, indicative both of minute size and low crystallinity. It was impossible to derive any information from the SAED patterns, not only on the lattice parameters but even on the values of interplanar spacings. In particular, samples consist of: a) anhedral grains, commonly associated in aggregates >50 nm in size and amorphous under electron diffraction, and b) elongate and thin lamellar flakes, 20–30 nm wide (Fig. 3a) and producing weak diffraction-rings. The latter particles are randomly oriented and usually form aggregates more than 50 nm across. High-magnification TEM images of the lamellar flakes show irregular lattice fringes, bent and polygonalized (Fig. 3b). More crystalline domains overlap in the projected, two-dimensional features. All these features are typical of chaotically assembled nanosized particles, possibly because of elastic deformation due to dehydration processes.

Individual grains have quite homogeneous chemical compositions. Both the anhedral grains and the elongate flakes show the presence of Ca, Fe, As and O as main elements (Table 2). The average Ca : Fe : As atomic proportions are 0.72 : 1.31 : 1. Comparable amounts of silicon and phosphorus invariably occur in the flakes, from 2.8 to 4.1 at.% and from 1.7 to 4.8 at.%, respectively. As minor contaminant phases, we detected a sulfate of calcium (as large euhedral crystals), a carbonate of calcium (as smaller anhedral crystals) and

TABLE 1. CHEMICAL COMPOSITION OF YUKONITE FROM GROTTA DELLA MONACA CAVE AND DAULTON MINE

	CaO	Fe$_2$O$_3$	As$_2$O$_3$	SiO$_2$	P$_2$O$_5$	H$_2$O	Total
Grotta della Monaca cave (EMPA data)							
1	13.4	31.9	39.9	2.3	0.2	12.3	100
2	13.8	30.9	41.0	2.1	0.2	12.1	100
3	12.9	29.7	38.4	2.0	0.1	16.9	100
4	13.6	32.0	39.7	2.3	0.2	12.2	100
5	12.9	33.5	36.9	2.4	0.1	14.3	100
6	12.4	32.9	38.3	2.5	0.1	13.9	100
7	12.6	32.7	37.5	2.5	0.2	14.6	100
Average	13.1	31.9	38.8	2.3	0.2	13.7	100
σ	0.5	1.3	1.4	0.2	0.1		
Grotta della Monaca cave (SEM–EDS data)							
1	10.4	32.4	50.1	0.4	2.4	4.2	100
2	11.0	31.2	44.3	0.4	2.5	10.5	100
3	12.9	30.4	47.5	0.4	0.5	8.3	100
4	12.5	26.9	37.1	2.0	-	21.4	100
5	12.9	29.1	39.2	1.9	-	16.9	100
6	13.1	26.8	37.8	2.0	-	20.2	100
7	11.9	29.3	31.4	2.9	0.4	24.1	100
8	12.4	28.5	43.8	0.5	0.7	14.1	100
9	13.4	31.1	46.9	0.5	0.7	7.3	100
Average	12.3	29.5	42.0	1.2	0.8	14.2	100
σ	1.0	1.9	6.0	1.0	1.0		
Daulton mine (SEM–EDS data)							
1	13.1	28.7	44.1	0.4	0.6	13.0	100
2	13.6	28.5	44.5	0.4	0.5	12.5	100
3	13.5	28.3	44.5	0.3	0.7	12.6	100
4	13.5	29.6	45.0	0.3	0.7	10.9	100
5	13.7	30.0	44.9	0.3	0.7	10.4	100
6	12.3	28.5	41.0	0.4	0.7	17.1	100
7	12.7	27.1	43.5	0.0	0.4	16.3	100
average	13.2	28.7	43.9	0.3	0.6	13.3	100
σ	0.5	0.9	1.4	0.1	0.1		

The amount of H$_2$O has been calculated as a difference, normalizing the totals to 100 wt.%.

TABLE 2. TEM–EDS CHEMICAL COMPOSITIONS OF YUKONITE FROM GROTTA DELLA MONACA CAVE AND DAULTON MINE

	Ca	Fe	As	Si	P
Grotta della Monaca cave, aggregate					
1	23.0	38.6	33.8	2.8	1.8
2	22.1	39.4	27.4	5.3	5.7
3	20.1	43.8	30.4	3.8	1.9
4	22.3	39.7	29.2	4.1	4.8
5	22.8	40.1	32.6	2.9	1.7
average	22.1	40.3	30.7	3.8	3.2
σ	1.2	2.0	2.6	1.0	1.9
Daulton mine, aggregate					
1	21.1	41.7	33.9	2.1	1.2
2	20.6	41.1	33.1	4.0	1.2
3	22.4	41.4	32.6	1.7	1.8
4	19.7	45.5	30.2	3.8	0.8
5	20.6	45.6	28.6	5.2	0.0
6	20.9	45.5	30.9	1.0	1.6
average	20.9	43.5	31.6	3.0	1.1
σ	0.9	2.3	2.0	1.6	0.6

Totals of Ca, Fe, As, Si and P have been normalized to 100%. Compositions are reported in atomic %.
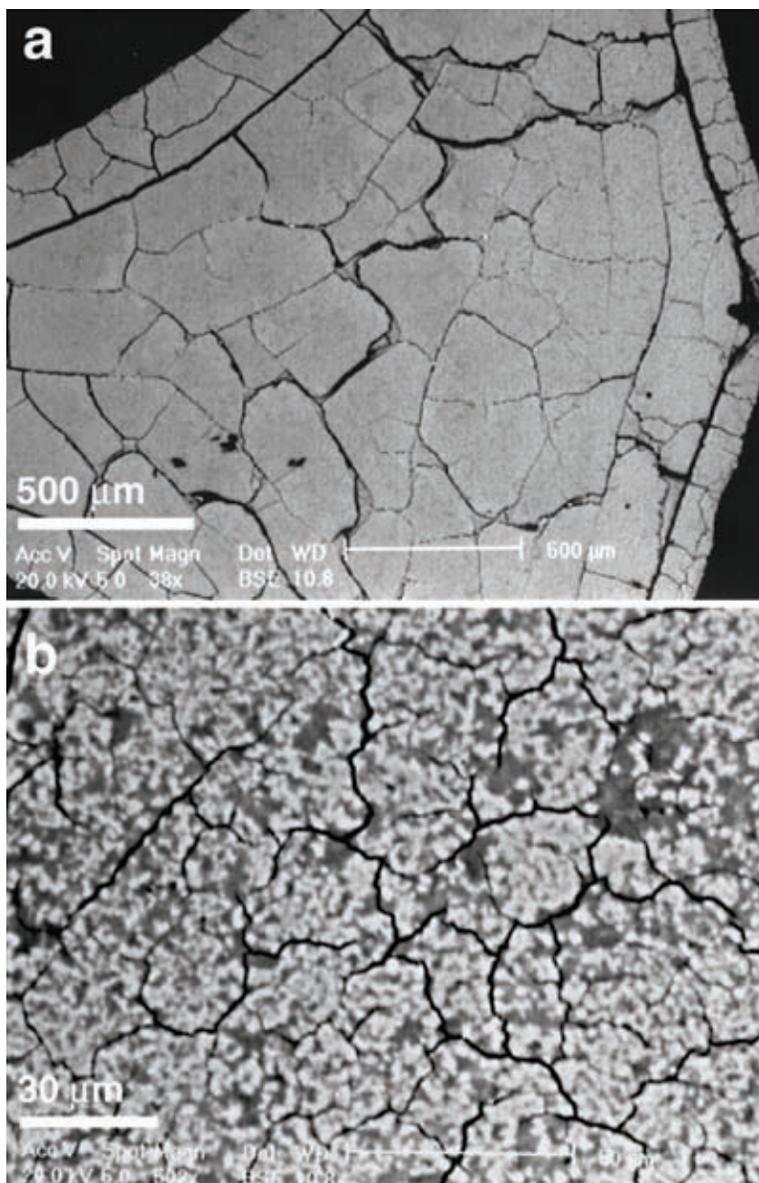
Fig. 2. (a) Back-scattered electron microphotograph of the Grotta della Monaca yukonite, showing dehydration-induced fractures, and (b) a granular texture, with close association of bright and dark grains.

an almost pure arsenate of Fe with a Fe/As ratio close to 1. The last phase, with mean atomic proportions of Ca 0.12, Fe 1.05, As 1.00, occasionally attains almost calcium-free proportions of Ca 0.03, Fe 1.01, As 1.00. In agreement with the X-ray powder-diffraction data, this phase is interpreted as scorodite, $Fe^{3+}AsO_4 \cdot 2H_2O$.

Yukonite from the Daulton mine was also found to consist of grain aggregates, with small, rare crystals of quartz. Most of the yukonite from the Daulton mine is amorphous under the electron beam. We cannot be sure if the mineral was originally amorphous or it became so during the observations, but the results of X-ray powder

data suggest the latter hypothesis. However, several thin plates showing a seemingly hexagonal symmetry and with clearly crystalline SAED pattern were observed sporadically.

FTIR spectroscopy

The spectra of yukonite from the Grotta della Monaca and Daulton mine are very similar (Fig. 4a). As expected, both patterns show an intense band at 860–800 cm^{-1}, which can be assigned to the AsO_4^{3-} stretching vibrations (*e.g.,* Ross 1974a). Considering that the sample from Grotta della Monaca contains scorodite impurities, this band reflects the overlapping modes of the arsenate group in both phases. Both samples show minor absorptions at 1132 and 1050 cm^{-1}; the latter, in particular, is resolved as a shoulder on the high-frequency side of the main arsenate band (Fig. 4a). These components can be assigned to the ν_3 stretching modes of the SO_4 (Ross 1974b) and PO_4 group (Ross 1974a), respectively. A rather broad absorption is

present at 1640 cm^{-1}, whereas a doublet at around 1430 cm^{-1} is observed in the Daulton mine spectrum; this latter feature is resolved as a shoulder at ~1395 cm^{-1} on the low-frequency side of the 1640 cm^{-1} band in the Grotta della Monaca specimen. The sharp bands around 1430 cm^{-1} in the Daulton mine material can be possibly assigned to carbonate groups (White 1974); however, an alternative explanation can be proposed (see below) for the broader 1395 cm^{-1} band in the Grotta della Monaca sample. The very broad and intense absorption centered around 3500 cm^{-1} is related to the presence of H_2O molecules or OH groups (or both); notably, it is "off-scale" in both spectra (Fig. 4a), in agreement with the high H_2O content of both samples (see below). For the samples of yukonite studied, this broad absorption can be assigned to H_2O, because it is associated with a well-defined band at 1640 cm^{-1} attributed to the bending mode of H_2O (*e.g.,* Ihinger *et al.* 1994). Assignment of the 3500 cm^{-1} band to molecular H_2O is also supported by the well-resolved component at 5170 cm^{-1}, which is related to the combination of the bending (ν_2) and
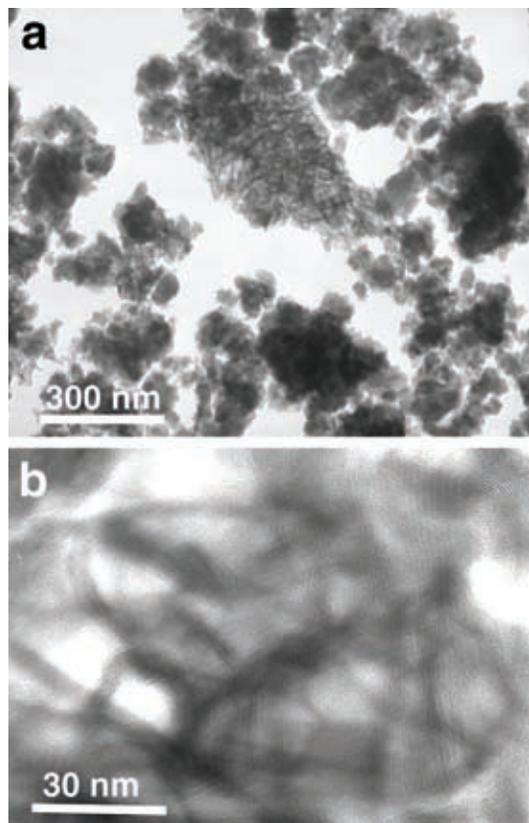
FIG. 3. (a) TEM image of the Grotta della Monaca yukonite, showing grains finely intermixed with an amorphous matrix; (b) irregular, bent and polygonized lattice fringes.
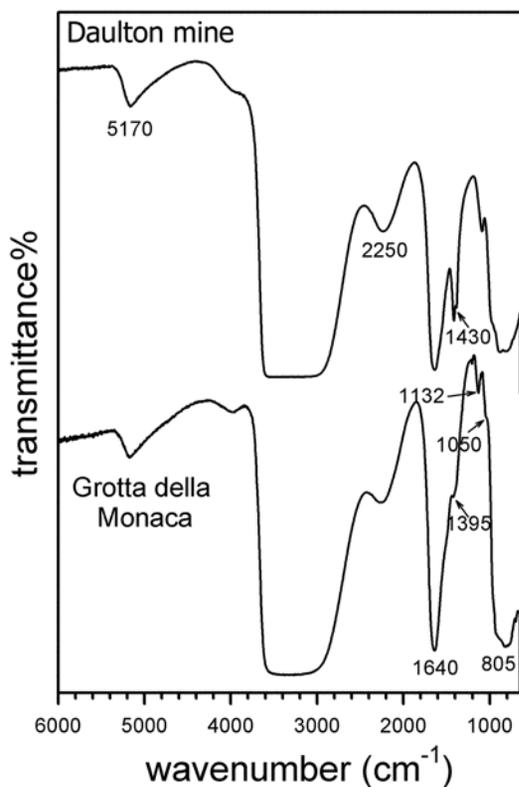
FIG. 4a. Unpolarized single-crystal FTIR spectra of yukonite from the Daulton mine, Yukon, Canada, and from Grotta della Monaca cave, collected on randomly oriented ~30 mm thick fragments.

stretching (ν_3) modes of H_2O (Ihinger *et al.* 1994). Both spectra (Fig. 4a) show a minor absorption at about 4000 cm^{-1}, the assignment for which is still debated. Its frequency is close to a combination involving an O–H stretching vibration coupled with a metal–oxygen stretching, as proposed for glasses (Ihinger *et al.* 1994) and various forms of hydrous silica (*e.g.,* Stone & Walrafen 1982). This being the case, the 4000 cm^{-1} band could indicate the presence of some OH groups in the samples examined, in addition to H_2O. Finally, both samples show a broad band at 2250 cm^{-1}, the assignment of which is discussed below.

In an attempt to resolve the extremely broad and multi-component absorption extending in the 3700–2500 cm^{-1} range, we collected several spectra for one fragment from Grotta della Monaca after annealing the sample at different temperatures (Fig. 4b). After collection of the room-temperature spectrum, the doubly-polished fragment was kept overnight at 110°C to remove the adsorbed moisture, then was annealed for one to two hours for each of the successive heating steps. Note that the broad band extending in the 3700 to 2500 cm^{-1} range is off-scale in all spectra collected for T ≤ 500°C. With increasing temperature, there is a
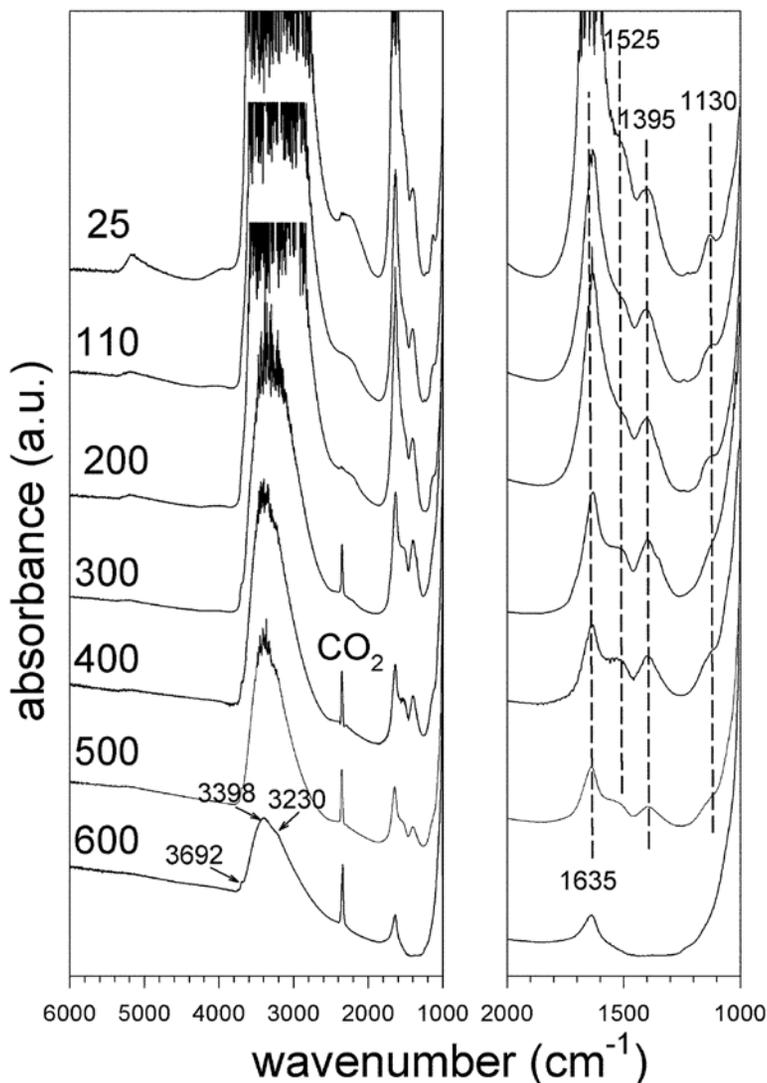
FIG. 4b. High-temperature FTIR spectra of yukonite from Grotta della Monaca. Temperature in °C. On the left side, the 2000–1000 cm^{-1} range is magnified for clarity.

significant decrease in intensity of the 3700–2500 cm^{-1} broad absorption, as well as of the 1640 and 5170 cm^{-1} bands, suggesting release of H_2O from the specimen. At 600°C, there is still a minor but resolvable amount of H_2O in the sample. Integration of the intensity of the 5170 cm^{-1} component suggests that heating the sample overnight at 110°C results in a loss of ~60% of the initial amount of H_2O present at 25°C; at 600°C, the amount of H_2O is 5–10% of the initial content. At 600°C, the main band is in scale (Fig. 4b), and two components can be resolved, centered at 3398 and 3230 cm^{-1}, respectively. Such low frequencies could indicate strongly hydrogen-bound H_2O molecules; however, such frequencies are also typical stretching frequencies of the ammonium group (*e.g.*, Busigny *et al*. 2003). Assignment of part of the absorption in the 3400–3200 cm^{-1} range to NH_4 is supported by the band at 1395 cm^{-1}, which can be assigned to the bending mode of NH_4 (*e.g.*, Busigny *et al*. 2003). With increasing temperature, this band decreases in intensity and disappears for T > 500–600°C (Fig. 4b), in agreement with the stability of the ammonium group in other minerals, such as ammonium-bearing analcime (Likhacheva *et al*. 2004).

A notable feature in Figure 4b is that for T ≥ 300°C, the unassigned band at 2240 cm^{-1} is replaced by an intense and extremely sharp absorption at 2346 cm^{-1}, which can be related without any doubt (Kolesov & Geiger 2003, Della Ventura *et al*. 2005, 2007) to the stretching vibration of CO_2. Inspection of the infrared spectroscopy literature shows that few molecular arrangements have absorption frequencies in the 2500–2000 cm^{-1} range, and these include organic C–H–N–O complexes (*e.g.,* Nakamoto 1962). The evolution of the 2240 cm^{-1} absorption as a function of T (Fig. 4b) thus suggests that probably poorly crystalline organic matter is trapped in the material examined and oxidizes with increasing temperature to give carbon dioxide. Additional modifications in the spectra also occur for increasing T; for example, the reduction in intensity of the 1640 cm^{-1} band, attributed to the release of H_2O from the sample, allows resolution of a new component

at 1525 cm^{-1}, whose assignment is not clear. We note, however, that the 1525 cm^{-1} band also vanishes for T > 500–600°C (Fig. 4b). The weak band at 1130 cm^{-1}, assigned to the SO_4 group (see above), seems to disappear for increasing T (Fig. 4b), in disagreement with the fact that the thermal analyses (see below) show that the sulfate group is released at 750–800°C. This feature is an artefact of the increasing broadening, due to increasing temperature, of the main arsenate band, which finally overlaps the weak sulfate component. Interestingly, at 600°C, a very weak but resolvable sharp component definitively shows up at 3692 cm^{-1}. This band, already observed as a shoulder in all spectra for T > 300°C, indicates the presence of OH groups in the sample studied. On the basis of the spectra of Figure 4b, it is not clear, however, if these hydroxyl groups are structurally bound in yukonite, or in the intermixed impurities.

Thermal analyses

The thermogravimetric (TG) curve of the Grotta della Monaca yukonite shows weight loss at 180°C, with a very strong endothermic reaction (Fig. 5), as is
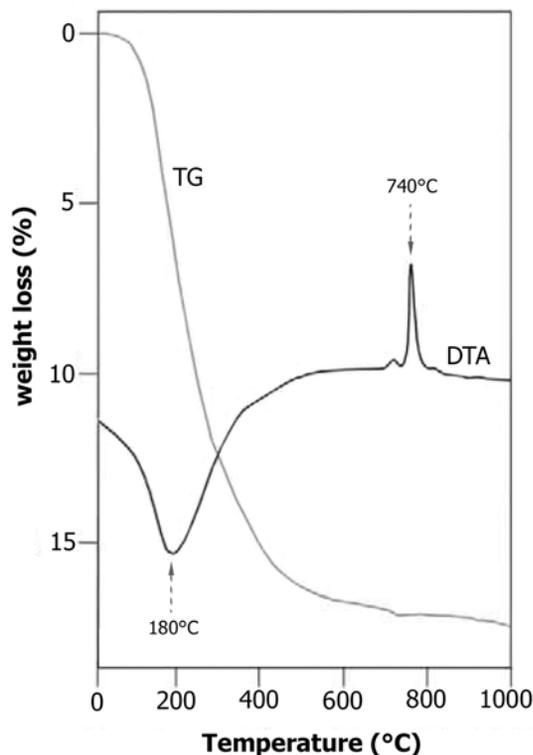
TABLE 3. X-RAY POWDER-DIFFRACTION DATA FOR THE YUKONITE AGGREGATE FROM GROTTA DELLA MONACA CAVE

d (Å)	I/I_0	Mineral	hkl	d (Å)	I/I_0	Mineral	hkl
15.690	100.0	Yuk	001	2.5903	17.9	Scd	213
5.640	34.9	Yuk/ Scd	110/ 111	2.5056	10.1	Scd	004,321
5.020	14.1	Scd	002	2.2456	8.5	Yuk	320
4.482	19.7	Scd	200,120	2.1427	6.9	Yuk	410
4.082	6.9	Scd	201,121	1.7642	8.6	Yuk	510
3.806	8.4	Scd	211	1.6417	14.9	Yuk	600
3.275	29.7	Yuk	300	1.5084	6.7	Yuk	610
3.177	26.2	Scd	212	1.4038	7.9	Yuk	700,530
3.053	15.0	Scd	131	1.2081	8.0	Yuk	720
2.9980	13.1	Scd	113	1.1060	10.0	Yuk	730
2.8083	28.7	Yuk	220	1.0847	11.3	Yuk	900
2.6843	21.4	Scd	203,123	1.0687	9.9	Yuk	820

Symbols: Yuk: yukonite, Scd: scorodite. The data for yukonite are indexed assuming a hexagonal unit-cell with a = 11.3, c = 15.7 Å.

FIG. 5. TG–DTA curves of the yukonite from Grotta della Monaca.

normal in the case of the release of molecular H_2O. A strong exothermic structural reorganization, without weight loss, occurs at 740°C. The total weight-loss ranges from 16.4 to 17.8 wt% in different samples; it is close to the H_2O contents reported elsewhere (Dunn 1982, Ross & Post 1997, Pieczka *et al.* 1998, Nishikawa *et al.* 2006).

XRD investigations

The powder-diffraction patterns given in Table 3 match the diffraction maxima previously reported for yukonite (Ross & Post 1997). In addition, sharp diffraction-maxima of scorodite, $FeAsO_4 \cdot 2H_2O$ (PDF 37–0468) are present in the Grotta della Monaca pattern, as can be clearly seen in Figure 6a, in which the X-ray-diffraction pattern is compared with that of a pure sample of yukonite from the Venus mine, Yukon Territory, Canada. In the sample from the type locality, the Daulton mine, Tagish Lake, some quartz was observed with the yukonite (Fig. 6b).

As already noticed by Ross & Post (1997), the powder-diffraction pattern of yukonite resembles that of minerals of the arseniosiderite group. In particular, all the observed diffraction-maxima (apart from the one at the lowest angle) correspond to *hk*0 reflections of arseniosiderite-type structure (0*kl* in the usual crystallographic setting of the group). The present choice of indices (Table 3) is consistent with the hexagonal setting of Nishikawa *et al.* (2006).

The basal spacing of yukonite, represented by the diffraction maximum at the lowest angle, is significantly larger than in arseniosiderite: between 14.1 and 15.7 Å in contrast to 8.8 Å in the latter (Ross & Post 1997). According to Ross & Post (1997), yukonite heated in air to 100°C acquires the basal spacing 11.1 Å, still significantly larger than arseniosiderite. The latter corresponds to the basal spacing found by Nishikawa *et al.* (2006) by electron diffraction. The larger value (15.7 Å) obtained for the Grotta della Monaca samples suggests a greater degree of hydration of the latter sample, or inclusion of some other interlayer molecules.

The general appearance of the patterns suggests a material of low crystallinity or high disorder or both. The resemblance to the arseniosiderite pattern can be explained if we assume the same topology and general composition of layers for yukonite. We note that layers of the arseniosiderite-type structures have a hexagonal
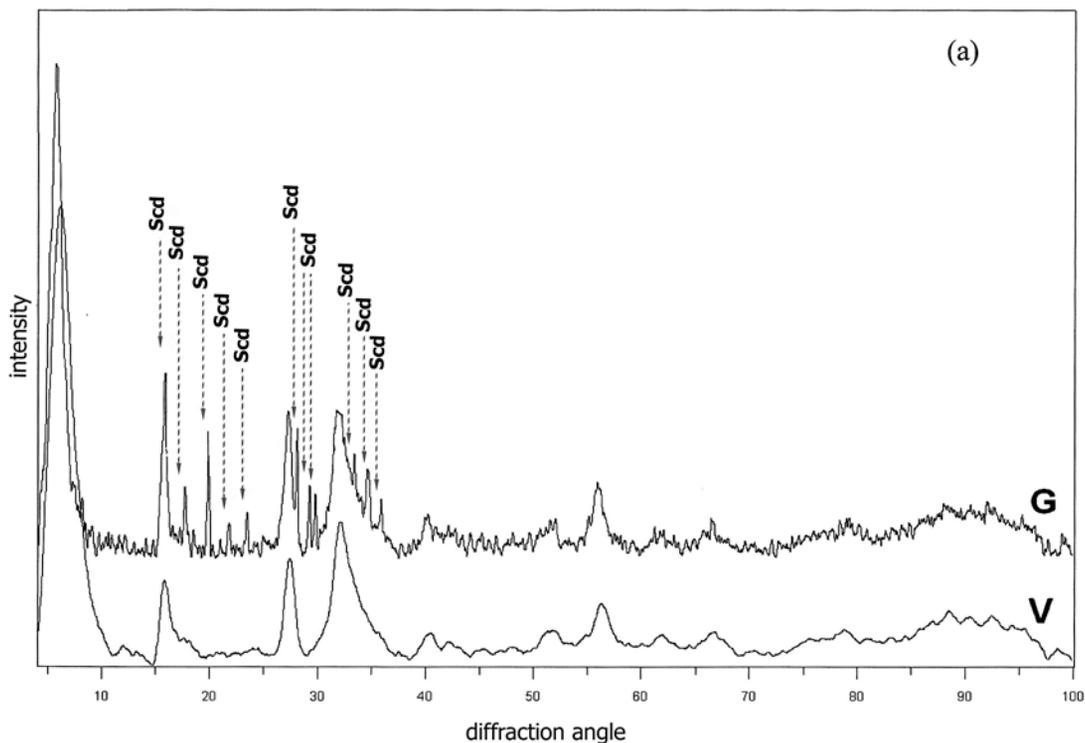
FIG. 6a. X-ray powder-diffraction patterns of yukonite from Grotta della Monaca (G) and Venus mine (V), Yukon Territory, Canada (ROM sample no. M37256, kindly placed at our disposal by the Royal Ontario Museum of Toronto). The sample from Grotta della Monaca contains some scorodite, whereas the one from the Venus mine has no additional phases.
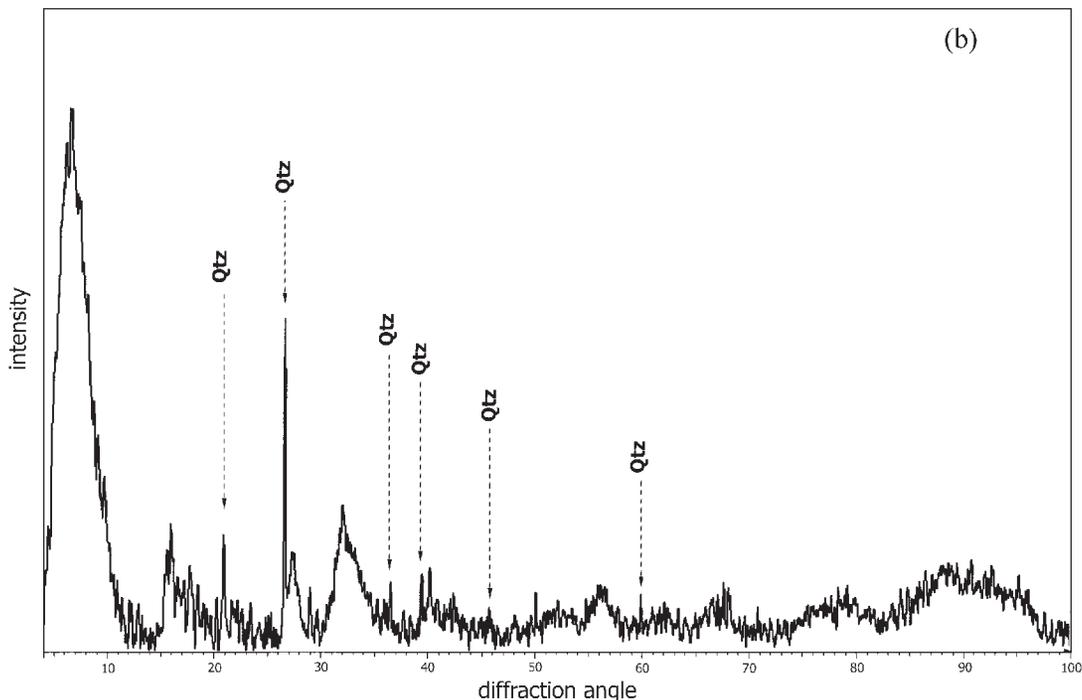
Fig. 6b.   X-ray powder-diffraction patterns of yukonite from the Daulton mine with quartz. Cu$K\alpha_1$ radiation, Guinier geometry. The background has been subtracted, and diagrams have been smoothed.

topology, the fundamental building block being formed by trigonal rings of edge-sharing [FeO_6] octahedra, centered by arsenate groups (Moore & Araki 1977). In accordance with this motif, we have chosen to index the diagram according to a hexagonal lattice, which is consistent with the least-ordered stacking of layers of the arseniosiderite type.

X-ray photoelectron spectroscopy observations

XPS spectroscopy was used to assess the oxidation state of iron in the material studied. Usually, the Fe2p XP spectra (Fig. 7) have a steeply rising background and broadened line-widths. These features are attributed to multiplet splitting and shake-up phenomena. In this study, the deconvolution of the iron spectrum has been carried out using the spectral parameters derived by McIntyre & Zetaruk (1977) from the spectra of two Fe oxides containing, respectively, only ferric iron or both ferrous and ferric iron. For yukonite, the curve fitting procedure of the Fe2p$_{3/2}$ component resulted into three peaks, corresponding to two chemical states of iron. The first [electron binding energy (BE) = 708.8 ± 0.1 eV] is assigned to ferrous iron, whereas the second

(BE = 711.3 ± 0.1 eV) and the third (BE = 714.2 ± 0.1 eV) are ascribed to ferric iron. From the area ratio of the above components, we determined that Fe^{2+}/Fe^{3+} is equal to 0.03.

Discussion and Conclusions

Our TEM investigations reveal that individual grains of yukonite, from both the Grotta della Monaca cave and the Daulton mine, are characterized by a very small size, ~20 nm in maximum dimension. These crystallites may eventually form assemblages of up to 300 nm, embedded within an amorphous matrix, and occasionally including additional well-crystallized minerals. In particular, scorodite has been detected as a contaminant in yukonite from the Grotta della Monaca cave.

Our SEM–EDS analyses of yukonite from the Grotta della Monaca cave and from the Daulton mine (Table 1) show a wide variation, in agreement with the range of compositions reported in the literature for yukonite from various occurrences. Owing to the very small grain-sizes, these analytical results are considered to indicate an average composition of yukonite plus matrix. Consequently, we conclude that the confu-
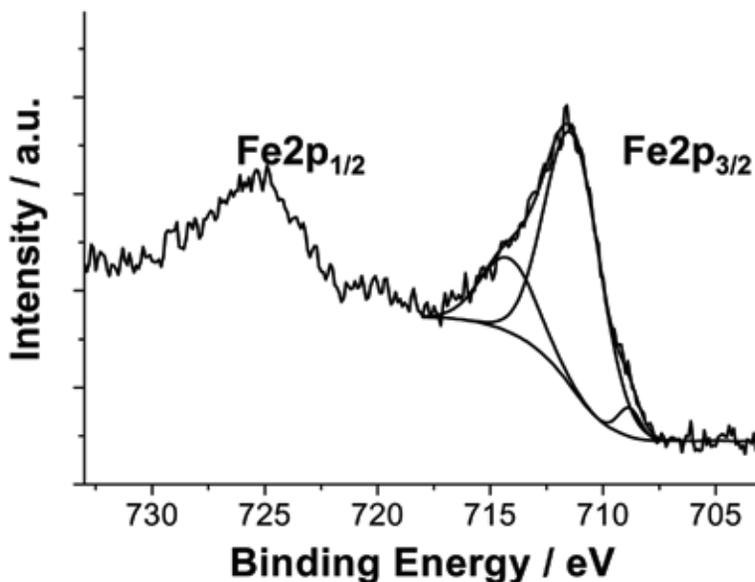
FIG. 7. XPS spectrum of yukonite from Grotta della Monaca.

sion about the formula of yukonite, reported in the literature for different occurrences and calculated from EMPA, EDS and wet-chemical analyses, may derive from analytical techniques unsuitable to achieve the required spatial resolution (<20 nm). For this reason, the following discussion on the mineralogical features of yukonite is carried out on the basis of TEM–EDS and X-ray absorption data only.

From the present TEM–EDS and XPS data, the following cation contents were calculated for the yukonite samples investigated in this work:

Grotta della Monaca cave:
$Ca_{1.76}Fe^{2+}_{0.09}Fe^{3+}_{3.12}(As_{2.44}Si_{0.30}P_{0.26})$

Daulton mine:
$Ca_{1.76}Fe^{2+}_{0.10}Fe^{3+}_{3.56}(As_{2.66}Si_{0.25}P_{0.09})$.
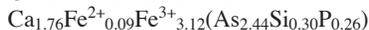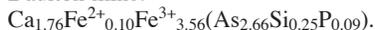
Taking into account the results of the thermal analysis, which suggest about 8 H_2O molecules, and the FTIR data, which show a variable presence of $(OH)^-$ groups, the previous composition can be rewritten as follows:

Grotta della Monaca cave: $Ca_{1.76}Fe^{2+}_{0.09}Fe^{3+}_{3.12}$
$[(As_{0.81}Si_{0.10}P_{0.09})O_4]_3(OH)_{3.76} \cdot 4H_2O$

Daulton mine: $Ca_{1.76}Fe^{2+}_{0.10}Fe^{3+}_{3.56}$
$[(As_{0.89}Si_{0.08}P_{0.03})O_4]_3(OH)_{5.16} \cdot 3H_2O$
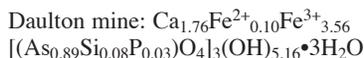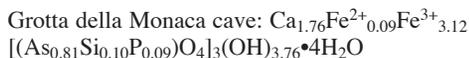
According to Nishikawa *et al.* (2006), the formulas have been calculated using the sum of the tetrahedrally coordinated cations normalized to 3, charge-balanced by change in the $OH:H_2O$ ratio.

These stoichiometries are very close to those reported for samples from Venus mine and Nalychevskie hot springs (Nishikawa *et al.* 2006). They also strongly recall the formula of arseniosiderite, $Ca_2Fe_3(AsO_4)_3O_2 \cdot 3H_2O$. The main difference is in the content of H_2O. A higher number of H_2O molecules correlates with the significantly larger interlayer spaces in yukonite, observed by XRD. We note that our FTIR results suggest as well the presence of organic molecules in yukonite; the TG loss and larger interlayer spacing may partly be due to them.

Another chemical difference between yukonite and arseniosiderite is a higher Fe : Ca ratio in the former. However, the ratio of the sum of Ca + Fe to As (+ Si + P) is in both cases 5:3. One may conclude that the surplus of Fe may be related to the replacement of As by Si in yukonite. The relation of yukonite to arseniosiderite remains an interesting question. Both chemical and XRD data show strong resemblances between the two phases, and one is tempted to propose that yukonite represents a semicrystalline aggregate of arseniosiderite-like layers poorly ordered and intermixed with amorphous material of variable composition.

Only rare flakes of yukonite from the Nalychevskie deposit produce single-crystal electron-diffraction

patterns (Nashikawa *et al.* 2006). Otherwise, TEM observations reveal a more poorly crystalline nature for both Grotta della Monaca and Daulton mine specimens, preventing us from obtaining any reliable lattice parameter. Actually, the yukonite from both Grotta della Monaca and Daulton mine consists of very finely inter-mixed distinct phases. The difference may be related with the chemical–physical conditions of genesis of yukonite from Nalychevskie, *i.e.,* deposition from hot springs (with a thermal gradient helping crystallization), undoubtedly different from occurrences where yukonite formed as an alteration product of As-rich minerals, such as arsenopyrite, köttigite and parasymplesite. Yukonite from the Grotta della Monaca cave also formed as an alteration of mixed sulfides occurring in an ore deposit connected with meta-ophiolites, by action of groundwater in an oxidizing environment (as confirmed by the occurrence of ferric iron). According to Paktunc *et al.* (2008), the formation of scorodite in the Grotta della Monaca cave could be interpreted as a phase transformation where a crystalline lattice is built at the expense of the amorphous component of yukonite.

The amount of P in the specimen from the Grotta della Monaca cave is connected to the particular environment of the cave, in which apatite and sampleite have been found in association with yukonite; the bat guano may be the source of ammonium and organic matter, trapped in the examined material, as the FTIR data show.

References

BACK, M.E. & MANDARINO, J.A. (2008): *Fleischer's Glossary of Mineral Species 2008*. The Mineralogical Record, Inc., Tucson, Arizona.

BONARDI, G., DE VIVO, B., GIUNTA, G., LIMA, A., PERRONE, V. & ZAPPETTA, A. (1982): Mineralizzazioni dell'Arco Calabro–Peloritano. Ipotesi generiche e quadro evolutivo. *Boll. Soc. Geol. It.* **101**, 141-155.

BUSIGNY, V., CARTIGNY, P., PHILIPPOT, P. & JAVOY, M. (2003): Ammonium quantification in muscovite by infrared spectroscopy. *Chem. Geol.* **198**, 21-31.

DELLA VENTURA, G., BELLATRECCIA, F. & BONACCORSI, E. (2005): CO_2 in minerals of the cancrinite–sodalite group: pitiglianoite. *Eur. J. Mineral.* **17**, 847-851.

DELLA VENTURA, G., BELLATRECCIA, F., PARODI, G.C., CÁMARA, F. & PICCININI, M. (2007): Single-crystal FTIR and X-ray study of vishnevite, ideally $[Na_6(SO_4)]$ $[Na_2(H_2O)_2](Si_6Al_6O_{24})$. *Am. Mineral.* **92**, 713-721.

DIMUCCIO, L.A., GARAVELLI, A., PINTO, D. & VURRO, F. (2005): Le Risorse Minerarie. *In* La Miniera Pre-Protostorica di Grotta della Monaca (Sant'Agata di Esaro – Cosenza). Centro regionale di Speleologia "Enzo de Medici", Roseto Capo Spulico, Calabria, Italy (37-41).

DUNN, P.J. (1982): New data for pitticite and a second occurence of yukonite at Sterling Hill, New Jersey. *Mineral. Mag.* **46**, 261-264.

GENIOLA, A. & VURRO, F. (2005): Presentazione. *In* La Miniera Pre-Protostorica di Grotta della Monaca (Sant'Agata di Esaro – Cosenza). Centro regionale di Speleologia "Enzo de Medici", Roseto Capo Spulico, Calabria, Italy (5).

IHINGER, P.D., HERVIG, R.L. & MCMILLAN, P.F. (1994): Analytical methods for volatiles in glasses. *In* Volatiles in Magmas (M.R. Carroll & J.R. Holloway, eds.). *Rev. Mineral.* **30**, 67-121.

JAMBOR, J.L. (1966): Re-examination of yukonite. *Can. Mineral.* **8**, 667.

KOLESOV, B.A. & GEIGER, C.A. (2003): Molecules in the SiO_2-clathrate melanophlogite: a single-crystal Raman study. *Am. Mineral.* **88**, 1364-1368.

LIKHACHEVA, A.YU., VENIAMINOV, S.A. & PAUKSHTIS, E.A. (2004): Thermal decomposition of NH_4-analcime. *Phys. Chem. Minerals* **31**, 306-312.

LORENZONI, S., ORSI, G. & ZANETTIN LORENZONI, E. (1982): Metallogenesis in the tectonic units and lithogenetic environments of Calabria (southern Italy). *Memorie di Scienze Geologiche* **35**, 411-428.

MCINTYRE, N.S. & ZETARUK, D.G. (1977): X-ray photoelectron spectroscopic studies of iron oxides. *Anal. Chem.* **49**, 1521-1529.

Moore, P.B. & Araki, T. (1977): Mitridatite: a remarkable octahedral sheet structure. *Mineral. Mag.* **41**, 527-528.

Nakamoto, K. (1962): *Infrared Spectra of Inorganic and Coordination Compounds*. J. Wiley & Sons, London, U.K.

Nickel, E.H. & Nichols, M.C. (1991): *Mineral Reference Manual*. Van Nostrand, New York, N.Y.

Nickel, E.H. & Nichols, M.C. (2007): IMA/CNMNC List of Mineral Names. http://www.geo.vu.nl/users/ima-cnmmn/MINERALlist.pdf

Nishikawa, O., Okrugin, V., Belkova, N., Saji, I., Shiraki, K. & Tazaki, K. (2006): Crystal symmetry and chemical composition of yukonite: TEM study of specimens collected from Nalychevskie hot springs, Kamchatka, Russia and from Venus mine, Yukon Territory, Canada. *Mineral. Mag.* **70**, 73-81.

Paktunc, D., Dutrizac, J. & Gertsman, V. (2008): Synthesis and phase transformation involving scorodite, ferric arsenate and arsenical ferrihydrite: implications for arsenic mobility. *Geochim. Cosmochim. Acta* **72**, 2649-2672.

Paktunc, D., Foster, A., Heald, S. & Laflamme, G. (2004): Speciation and characterization of arsenic in gold ores and cyanidation tailings using X-ray absorption spectroscopy. *Geochim. Cosmochim. Acta* **68**, 969-983.

Paktunc, D., Foster, A. & Laflamme, G. (2003): Speciation and characterization of arsenic in Ketza River mine tailings using X-ray absorption spectroscopy. *Envir. Sci. Tech.* **37**, 2067-2074.

Pieczka, A., Gołębiowska, B. & Franus, W. (1998): Yukonite, a rare Ca–Fe arsenate, from Rędziny (Sudetes, Poland). *Eur. J. Mineral.* **10**, 1367-1370.

Ross, D.R. & Post, J.E. (1997): New data on yukonite. *Powder Diffraction* **12**, 113-116.

Ross, S.D. (1974a): Phosphates and other oxy-anions of group V. *In* The Infrared Spectra of Minerals (V.C. Farmer, ed.). The Mineralogical Society, London, U.K. (Monograph 4, 383-422).

Ross, S.D. (1974b): Sulphates and other oxy-anions of group VI. *In* The Infrared Spectra of Minerals (V.C. Farmer, ed.). The Mineralogical Society, London, U.K. (Monograph 4, 423-444).

Stone, J. & Walrafen, G.E. (1982): Overtone vibrations of OH groups in fused silica optical fibers. *J. Chem. Phys.* **76**, 1712-1722.

Tyrrell, J.B. & Graham, R.P.D. (1913): Yukonite, a new hydrous arsenate of iron and calcium, from Tagish Lake, Yukon Territory, Canada: with a note on the associated symplesite. *Trans. R. Soc. Can., Sect. 4,* **7**, 13-18.

White, W.B. (1974): The carbonate minerals. *In* The Infrared Spectra of Minerals (V.C. Farmer, ed.). The Mineralogical Society, London, U.K. (Monograph 4, 227-284).